CODEE Journal

Volume 15 Article 1

3-11-2022

Human Impact on Planetary Temperature and Glacial Volume: Extending a Toy Climate Model to a New Millennium

Samantha Secor
California State Polytechnic University, Pomona

Jennifer Switkes
California State Polytechnic University, Pomona

Human Impact on Planetary Temperature and Glacial Volume: Extending a Toy Climate Model to a New Millennium

Samantha Secor and Jennifer Switkes
California Polytechnic University, Pomona

Keywords: Climate Change, System of Differential Equations
Manuscript received on March 18, 2021; published on March 12, 2022.

Abstract: Starting with a toy climate model from the literature, we employ a system of two nonlinear differential equations to model the reciprocal effects of the average temperature and the percentage of glacial volume on Earth. In the literature, this model is used to demonstrate the potential for a stable periodic orbit over a long time span in the form of an attracting limit cycle. In the roughly twenty five years since this model appeared in the literature, the effects of global warming and human-impacted climate change have become much more well known and apparent. We demonstrate modification of initial conditions to understand how human activity could affect the model results. Although we too see the attracting limit cycle that yields a periodic orbit, we demonstrate that small perturbations in initial conditions can lead to extreme outcomes due to the presence of a nearby saddle point. We simulate the results over time to to highlight the critical nature of perturbations that in effect change the initial conditions and to determine how soon drastic climate events might take place.

1 Introduction

Climate change is a term that in recent decades has become widely used around the world. It impacts us everyday, whether we are aware of it or not. Two effects and reciprocal causes that are often associated with climate change are melting glaciers and rising Earth temperatures. Water—in any of its phases—plays a unique role in Earth's system. It has been said often that glaciers are sentinels of climate change. Extreme heat, droughts, rising sea level, and severe storms are just some of the effects from small changes in temperature. Death Valley, California, U.S.A., recently recorded a global high temperature on August 16, 2020, at 130° Fahrenheit (54° Celsius), an anecdote and note of caution worth reflection.

In recent decades, the literature has become rich with models of global warming, taking various approaches to the problem and coming from a variety of disciplines and

interdisciplinary work. Here, we will explore and expand upon the results provided by a toy climate model. Toy climate models, while deep simplifications, nonetheless can provide important insight into real issues, processes, and outcomes. One interesting set of toy climate models explores what has become known as Daisyworld; see [8] for an overview and review of this set of models. The model structure is a system of nonlinear differential equations. The basic concept is a planet covered by two types of daisies, with different albedo values, hence affecting planetary temperature, in turn affecting the growth or shrinkage of the daisy patches. These models, the concept of which was initially developed by [7], support (and in some later cases critique) the idea that the Earth system self-regulates through feedback mechanisms in a manner that returns it to healthy stability. An interesting follow-up work by [4] provides a level of warning about the outcomes to Daisyworld when regulation begins to break down.

A collection of models developed by Saltzman and others around the same time uses a different framework and analyzes different aspects of the Earth system to include and explore, without the idea of Gaia-like self-regulation, ideas of feedback that produces limit cycles; see [3]. In brief this collection of models, also using nonlinear differential equations, examines the feedback mechanisms between sea ice extent, deep ocean temperature, and atmospheric carbon dioxide. A later paper by [1] develops a toy climate model consisting of components for ocean, land, glacier, and sea ice. Kroll's model follows from the heritage provided by Saltzman in a group of related articles, and also builds from the cluster of papers mentioned next, while suggesting the possibility and plausibility of a strong underlying natural period. We will argue later for further examination of this position in the presence of significant human impact on climate conditions.

Continuing in the tradition of earlier toy climate models, we build off of a model initially developed by Posmentier and examined further by Toner and Kirwan [2, 5, 6]. This toy climate model, again a system of nonlinear differential equations, explores the two factors of glacier coverage and average radiation temperature to understand how they relate to climate change and how human activity changes their behavior. In Section 2, we provide a concise overview of the model as presented in [6]. In Section 3, we highlight graphical features of the model; these were mentioned in [6] but here we underscore their importance in connection with exploration of human impact. In Section 4, we re-envision the results of [6] from a contemporary perspective in regard to human-caused climate change. Finally, in Section 5, we discuss our results and conclusions.

2 The Toy Climate Model of Toner and Kirwan (1994)

We begin by reviewing the toy climate model as presented in [6]. The model governs the behavior of two variables: $G(t)$, the percent of the planet covered by glaciation as a function of time, and $T(t)$, the average radiation temperature of the planet as a function of time, and is formulated as a system of two nonlinear differential equations:

$$\dot{G} = RG(1-G) - AG - BT + C, \tag{2.1}$$

$$\dot{T} = L\dot{G} - KT^4 + F(1-G). \tag{2.2}$$

Differentiation is with respect to time. The parameter R represents the rate of evaporation. The parameter L represents the latent heat associated with when the glacier freezes water, in turn growing the size of the glacier. The parameter K is a modified Stefan-Boltzmann constant. The parameter F is a function of the albedo associated with the percentage of the planet's surface that is not covered by glaciation. The parameters A, B, and C are used to fit the model. Throughout this section we summarize [6] as we move rapidly from the initial variables through two changes of variables that help us analyze and explore the system. First we summarize the equilibrium solutions of system (2.1)–(2.2) as found by [6].

2.1 Indexing Equilibria

In matrix form, system (2.1)–(2.2) is equivalent to

$$\begin{bmatrix} 1 & 0 \\ -L & 1 \end{bmatrix} \begin{bmatrix} \dot{G} \\ \dot{T} \end{bmatrix} = \begin{bmatrix} RG(1-G) - AG - BT + C \\ -KT^4 + F(1-G) \end{bmatrix}. \tag{2.3}$$

Letting $\dot{G} = \dot{T} = 0$ in the second row of (2.3),

$$G = 1 - \frac{K}{F}T^4.$$

Introducing with [6] the new parameter $\kappa = K/F$,

$$G = 1 - \kappa T^4. \tag{2.4}$$

Focusing on the first row of (2.3) with $\dot{G} = 0$, and using equation (2.4),

$$RG(1-G) - AG - BT + C = 0,$$
$$-R\kappa^2 T^8 + (A\kappa + R\kappa)T^4 - BT + C - A = 0.$$

Solving for C by assuming an equilibrium temperature, T_e,

$$C = R\kappa^2 T_e^8 - (A\kappa + R\kappa)T_e^4 + BT_e + A.$$

Thus,

$$-R\kappa^2 T^8 + R\kappa^2 T_e^8 + R\kappa T^4 - R\kappa T_e^4 + A\kappa T^4 - A\kappa T_e^4 - BT + BT_e = 0$$

which factors as

$$\begin{aligned}(T-T_e)\Big[&-R\kappa^2 T^7 - T_e R\kappa^2 T^6 - T_e^2 R\kappa^2 T^5 - T_e^3 R\kappa^2 T^4 + \kappa(R - R\kappa T_e^4 + A)T^3 \\ &+T_e\kappa(R - R\kappa T_e^4 + A)T^2 + T_e^2\kappa(R - R\kappa T_e^4 + A)T - R\kappa^2 T_e^7 + T_e^3 A\kappa + T_e^3 R\kappa - B\Big] = 0.\end{aligned} \tag{2.5}$$

The left-hand side is an eighth-degree polynomial so there are many other roots that are equilibrium solutions in addition to the equilibrium temperature, T_e. These solutions will be discussed in the next sections, where we will find that there is only one other real-valued equilibrium, a saddle. Factoring as we have in (2.5), we index the equilibrium solutions of (2.1)–(2.2) as

$$\begin{bmatrix} G_i \\ T_i \end{bmatrix} = \begin{bmatrix} 1 - \kappa T_i^4 \\ T_i \end{bmatrix} \tag{2.6}$$

where T_i is a solution of (2.5) for $i = 1, 2, \ldots, 8$ and $T_1 = T_e$ [6].

Next, with [6], we apply a first transformation to system (2.1)–(2.2).

2.2 y-coordinate Transformation

With [6], we translate equilibrium $i = 1$ in (2.6) corresponding to $G_1 = G_e$, $T_1 = T_e$ to the origin $y_1 = 0$, $y_2 = 0$:

$$G = y_1 + 1 - \kappa T_e^4, \qquad T = y_2 + T_e.$$

Incorporating C into system (2.1)–(2.2) and making the change of variables from (G, T) to (y_1, y_2),

$$\begin{bmatrix} \dot{y}_1 \\ \dot{y}_2 \end{bmatrix} = \begin{bmatrix} M(1) \\ M(2) \end{bmatrix}$$

where $M(1)$ and $M(2)$ are defined by

$$\begin{aligned} M(1) &= -Ay_1 - Ry_1 + 2\kappa RT_e^4 y_1 - Ry_1^2 - By_2, \\ M(2) &= -Fy_1 - ALy_1 - LRy_1 + 2\kappa LRT_e^4 y_1 \\ &\quad - LRy_1^2 - BLy_2 - 4F\kappa T_e^3 y_2 - 6F\kappa T_e^2 y_2^2 - 4F\kappa T_e y_2^3 - F\kappa y_2^4. \end{aligned}$$

Setting

$$\mathbf{A} = \begin{bmatrix} 2R\kappa T_e^4 - R - A & -B \\ 2LR\kappa T_e^4 - LR - LA - F & -LB - 4\kappa F T_e^3 \end{bmatrix}$$

and

$$\mathbf{f}(\mathbf{y}) = \begin{bmatrix} -Ry_1^2 \\ -LRy_1^2 - \kappa F y_2^4 - 4\kappa F y_2^3 T_e - 6\kappa F y_2^2 T_e^2 \end{bmatrix},$$

system (2.1)–(2.2) becomes

$$\dot{\mathbf{y}} = \mathbf{A}\mathbf{y} + \mathbf{f}(\mathbf{y}), \tag{2.7}$$

as given in [6].

Now, we apply a second transformation.

2.3 u-coordinate Transformation

With [6], we apply a transformation onto (2.7) of the following:

$$\mathbf{y} = \mathbf{P}\mathbf{u} \tag{2.8}$$

where $\mathbf{P}$ is a nonsingular matrix such that

$$\mathbf{P}^{-1}\mathbf{A}\mathbf{P} = \begin{bmatrix} \alpha & \omega \\ -\omega & \alpha \end{bmatrix}.$$

Notice that the linear part of the differential equation for u thus becomes $\dot{\mathbf{u}} = (\mathbf{P}^{-1}\mathbf{A}\mathbf{P})\mathbf{u}$, with $\mathbf{P}^{-1}\mathbf{A}\mathbf{P}$ having eigenvalues $\alpha \pm \omega i$. As shown in [6],

$$\begin{aligned} \mathbf{P} = &\begin{bmatrix} -4\kappa F^2 T_e^3 & 0 \\ F^2 & 0 \end{bmatrix} + \alpha \begin{bmatrix} 4L\kappa F T_e^3 - F & 0 \\ -2LF & 0 \end{bmatrix} \\ &+ \omega \begin{bmatrix} 0 & -F(1 + 4\kappa T_e^3 L) \\ 0 & 0 \end{bmatrix} + (\alpha^2 + \omega^2) \begin{bmatrix} L & 0 \\ L^2 & 0 \end{bmatrix}. \end{aligned}$$

As given in [6],we let $\alpha = \lambda\omega$ and consider $|\lambda| << 1$. This makes α small in magnitude compared to ω, giving almost-periodic behavior in the linear system. We also transform the time variable t to τ, given by $\tau = \omega t$. For clarity, note that

$$\dot{\mathbf{u}} \equiv \frac{d\mathbf{u}}{dt}, \qquad \mathbf{u}' \equiv \frac{d\mathbf{u}}{d\tau}.$$

Under this change of variables, system (2.7) becomes

$$\mathbf{u}' = \begin{bmatrix} 0 & 1 \\ -1 & 0 \end{bmatrix} \mathbf{u} + \lambda \mathbf{u} + \frac{\mathbf{1}}{\omega} \mathbf{P}^{-1} \mathbf{f}(\mathbf{P}\mathbf{u}).$$

We set

$$\mathbf{g}(\mathbf{u}) = \lambda \mathbf{u} + \frac{\mathbf{1}}{\omega} \mathbf{P}^{-1} \mathbf{f}(\mathbf{P}\mathbf{u})$$

obtaining

$$\mathbf{u}' = \begin{bmatrix} 0 & 1 \\ -1 & 0 \end{bmatrix} \mathbf{u} + \mathbf{g}(\mathbf{u}) \tag{2.9}$$

Name	Description	Value	Units
G	Percent of the planet's surface covered by glaciation	$G_e = 9.7$	%
T	Average temperature of the planet	$T_e = 246$	**K**
A	Proportional to melting from glacial movement	-0.0049	**1/year**
B	Proportional to melting from temperature increase	-7.2493×10^{-5}	**1/(K· year)**
C	Planetary constant given by Toner & Kirwan 1994	-0.0183	**1/year**
c_3	Soft parameter given by Toner & Kirwan 1994	-0.0021	**K/year**^{4}
F	Proportional to albedo of bare planet surface	0.43395	**K/year**
K	Proportional to black-body emissivity	1.07×10^{-10}	**1/(K**^{3}**·year)**
L	Proportional to the latent heat of evaporation	20	**K**
R	Proportional to the evaporation rate	8×10^{-5}	**1/year**
κ	Used for simplification given by Toner & Kirwan 1994	2.46572×10^{-10}	**1/K**^{4}
α	Determines the spiral of the periodic orbits	6.7134×10^{-9}	**1/year**
ω	Determines rotational period of the periodic orbits	3.1416×10^{-4}	**1/year**
λ	Used for stability analysis	2.1369×10^{-5}	Unitless
a	Radius of the periodic orbit in u coordinates	0.1	**year**^{2}**/K**
A	Matrix given by Toner & Kirwan 1994	$\begin{bmatrix} 0.0082 & 0.0001 \\ -0.5614 & -0.0082 \end{bmatrix}$	**1/year**
P	Matrix given by Toner & Kirwan 1994	$\begin{bmatrix} -0.0028 & -0.0002 \\ 0.1884 & 0 \end{bmatrix}$	**K/year**^{2}

Table 1: Parameter values and their descriptions.

as given in [6]. In the linear portion of this system given by omitting $\mathbf{g}(\mathbf{u})$, the parameter ω governs the rotational period $2\pi/\omega$ of periodic orbits in the time variable t. System (2.9) is convenient for further analysis, as pointed out by [6].

3 Graphical Features of the Toner and Kirwan Model (1994)

Having surveyed briefly [6], we now enter into the explorations that form the heart of our work. We begin by running numerical simulations of the Toner and Kirwan Model in MATLAB, using the set of parameter values given in Table 1. We use constant parameters, but further work can be done to allow parameters to vary with time.

3.1 Equilibrium Climate Conditions

There are eight equilibrium solutions in each of the systems (2.1)–(2.2), (2.7), and (2.9), which are given in Table 2. In each system however, only two equilibrium solutions are real-valued and the rest are complex conjugate pairs. For example, (G_1, T_1) and (G_2, T_2) are the real-valued equilibria in the (G, T) system. Note that G_1 corresponds to $G_e = 9.7\%$ glaciation, in agreement with approximate glacial levels. Similarly, T_1 corresponds to $T_e = 246$ K, an approximate value for Earth's average radiation temperature. The equilibrium (G_1, T_1) is an unstable source (with a limit cycle around it, as we will see later). We will refer to (G_1, T_1) as the bounded equilibrium. The equilibrium (G_2, T_2) is a saddle. These behaviors between (G_1, T_1) and (G_2, T_2), the bounded and saddle equilibria, respectively, translate into the y-coordinate and u-coordinate systems. In the next sections, we aim to understand how sensitive each system is to minor and major changes in initial conditions.

Equilibrium Type	**Equilibrium Name**	**Equilibrium Value**
Bounded	(G_1, T_1)	$(0.097006, 246)$
Saddle	(G_2, T_2)	$(0.089702, 246.496)$
Complex Conjugate Pair	(G_3, T_3) and (G_4, T_4)	$(50.351 \pm 10.462i, -499.739 \pm 450.088i)$
Complex Conjugate Pair	(G_5, T_5) and (G_6, T_6)	$(7.257 \pm 7.149i, -239.999 \pm 372.432i)$
Complex Conjugate Pair	(G_7, T_7) and (G_8, T_8)	$(65.731 \pm 6.753i, 493.491 \pm 519.833i)$
Bounded	(y_{11}, y_{12})	$(0, 0)$
Saddle	(y_{21}, y_{22})	$(-0.007304, 0.495951)$
Complex Conjugate Pair	(y_{31}, y_{32}) and (y_{41}, y_{42})	$(50.253 \pm 10.462i, -745.739 \pm 450.088i)$
Complex Conjugate Pair	(y_{51}, y_{52}) and (y_{61}, y_{62})	$(65.634 \pm 6.753i, 247.491 \pm 519.833i)$
Complex Conjugate Pair	$(y_{71}, y_{72})$and (y_{81}, y_{82})	$(7.161 \pm 7.149i, -485.999 \pm 372.432i)$
Bounded	(u_{11}, u_{12})	$(0, 0)$
Saddle	(u_{21}, u_{22})	$(2.633112, 0.163132)$
Complex Conjugate Pair	(u_{31}, u_{32}) and (u_{41}, u_{42})	$(1314 \pm 2760i, -392737 \pm 81532i)$
Complex Conjugate Pair	(u_{51}, u_{52}) and (u_{61}, u_{62})	$(-3959 \pm 2390i, -222912 \pm 96757i)$
Complex Conjugate Pair	(u_{71}, u_{72}) and (u_{81}, u_{82})	$(-2580 \pm 1,977i, -178 \pm 9563i)$

Table 2: All equilibrium solutions in (G, T), y, and u coordinates.

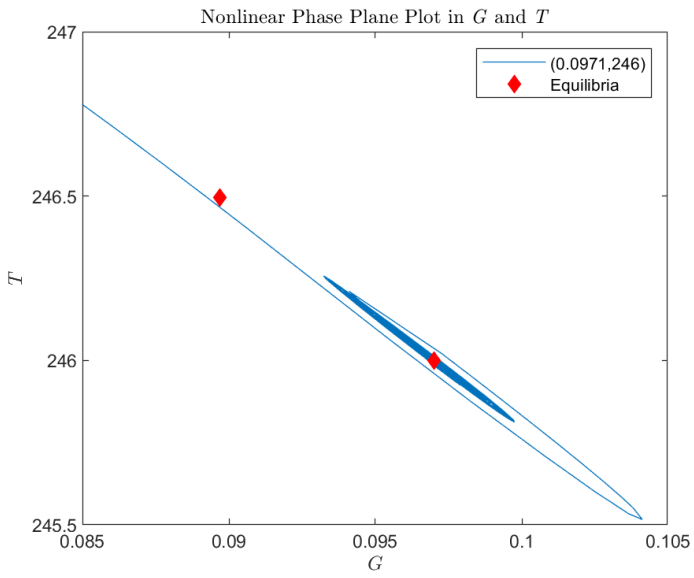

Figure 1: Trajectories in the G and T phase plane for the nonlinear system (2.1) and (2.2).

3.2 Glaciation Percentage and Average Temperature

The non-linear system (2.7) in y-coordinates yields the phase plane plot shown in Figure 1. Curves spiral from the equilibrium at (G_1, T_1) which is approximately 9.7% glacial volume and 246 K average radiation temperature. Note that it is hard to thoroughly identify any type of periodic or unstable behavior, which is why Toner and Kirwan conducted the first transformation into y-coordinates. Although this transformation is simply a translation, it centers the bounded equilibrium at $(y_{11}, y_{12}) = (0, 0)$, as shown in Table 2 and in Figure 2.

Once the y-coordinate transformation is conducted however, it is still very hard to understand behavior using this system. In the u-coordinate system, it is easier to visually identify the curves and understand the classification of the equilibrium points. The non-linear system in (2.9) yields the plot in Figure 3, showing the two equilibria we are analyzing. We see clearly the bounded equilibrium, an unstable source with a limit cycle around it; and the saddle equilibrium. The saddle equilibrium at about $(u_1, u_2) = (2.63, 0.16)$ is causing certain trajectories to get pulled away from $(0, 0)$. We can also see concentric curves about $(0, 0)$, but this equilibrium point is a little harder to categorize.

From analyzing these plots, we can identify two unique and important features in the phase plane for the Toner and Kirwan Model. The first is the presence of a limit cycle around the unstable source given by the bounded equilibrium. It is the presence of this limit cycle that provides hope for moderate climate cycles that are beneficial to human survival. The second is the unique structure of the separatrices governing the impacts of the saddle and the unstable source and separating types of behavior based on initial condition. It is the presence of these curves that provides a hint of the danger ahead when we turn our attention to human impact on climate change. We next explore these two important features and begin to tie our results directly to issues of climate change.

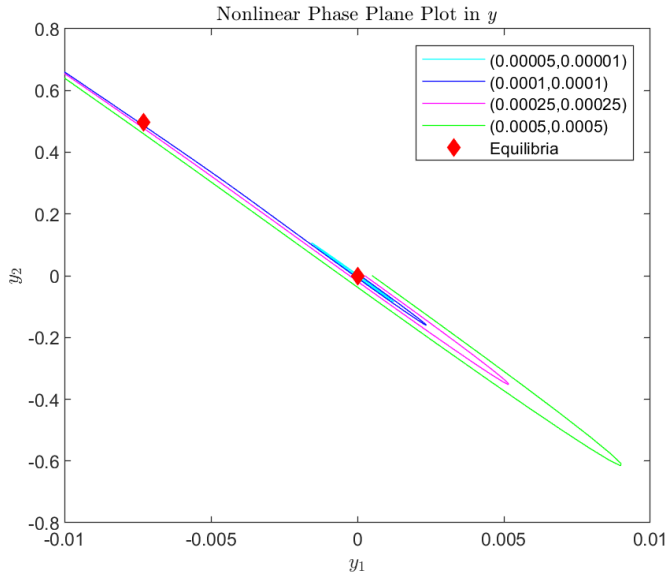

Figure 2: Trajectories in the y_1 and y_2 phase plane for the nonlinear system (2.7).

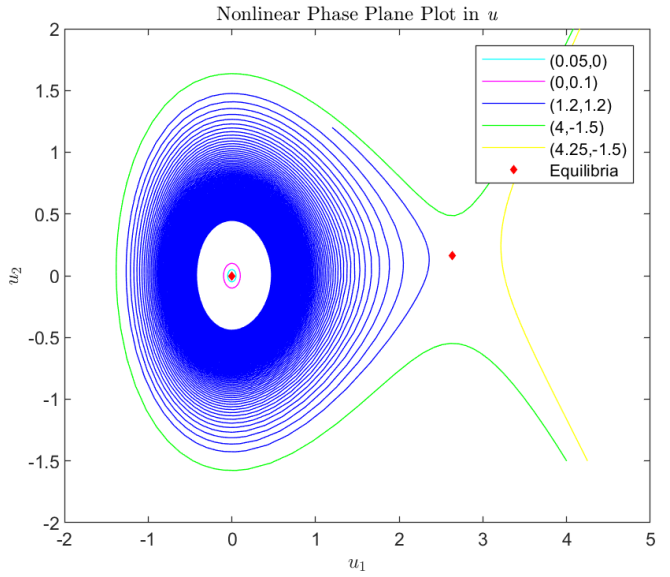

Figure 3: Trajectories in the u_1 and u_2 phase plane for the nonlinear system (2.9).

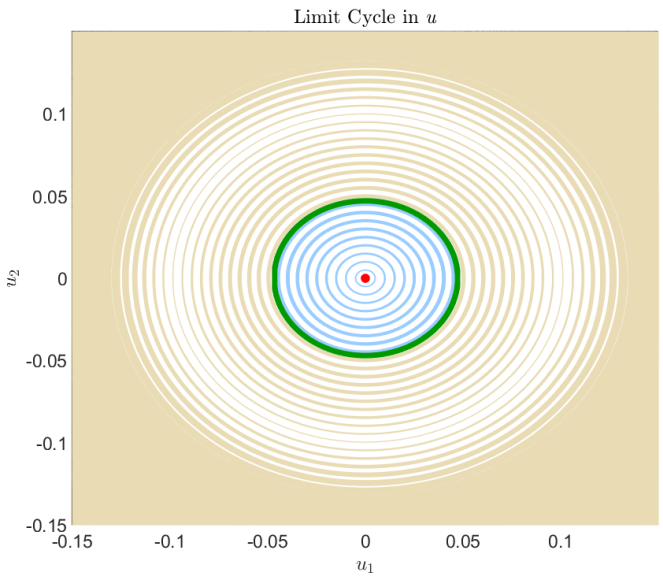

Figure 4: Multiple initial conditions plotted to numerically find the limit cycle around the bounded equilibrium, $(0, 0)$.

3.3 The Limit Cycle: Our Hope in Climate Change

In order to solidify our visual identification of a limit cycle, we will plot points around the equilibrium $(0, 0)$ to understand numerically the behavior for initial conditions sufficiently close to and far from the equilibrium for the non-linear system in (2.9). Figure 4 helps confirm our observation that a limit cycle exists. It appears that the limit cycle exists in (u_1, u_2) coordinates that pass through roughly the point $(0.0467, 0)$. Note that in this plot, all yellow initial conditions will result in eventually aligning with the limit cycle, shown in green. This is stable behavior. The blue region shows initial conditions which stem from the unstable, bounded equilibrium point, and flows to the limit cycle.

Recall an earlier comment that periodic orbits in (u_1, u_2) have a rotational period of $2\pi/\omega$. Using $\omega = 2\pi/20,000$ and $\tau = \omega t$, a limit cycle here would have a period of $20,000$ years. Numerically, we show that the periodic orbit for this limit cycle is between $19,826$ to $20,235$ years, which solidifies the argument that a limit cycle exists here.

Speaking more mathematically, the bounded equilibrium at $(0, 0)$ is classified as an unstable spiral, as the linearized system about this point has a complex conjugate pair of eigenvalues with (slightly) positive real part. On the other hand, close to but outside of the radius of the apparent limit cycle, the vector field for the nonlinear system points inward towards the apparent limit cycle. An informal application of the Poincare-Bendixson Theorem, under the well-founded assumption that there is only one closed curve here, therefore yields the existence of a limit cycle.

In real-world terms, the limit cycle represents our hope in climate change because this is the limit at which the temperature and glacial volume changes are minimized and fixed. Initial conditions that head toward the bounded equilibrium in u-coordinates, namely $(0, 0)$, translate into minor changes within G and T in terms of system (1) and (2). This

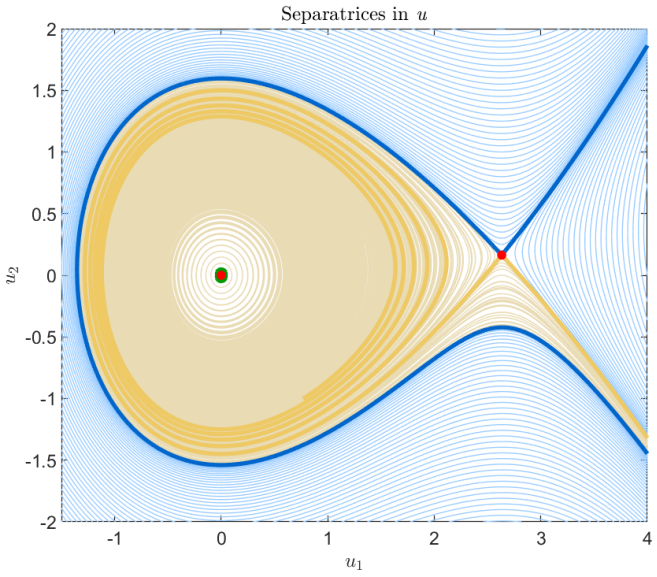

Figure 5: Multiple initial conditions plotted to graphically display stabilities around the separatrices.

means if the Earth has levels of glacial volume and temperatures that head toward the limit cycle, the Earth will see natural cyclic changes in both of these variables, but it will not be drastic enough to lead to significant change. We will continue to explore these behaviors in Section 4.

3.4 The Separatrices: Disaster in the Making

Now that we have explored the limit cycle, we want to explore more evidence of separatrices in our model. We have plotted approximately where the separatrices are located in u-coordinates, given in Figure 5. Note that all yellow initial conditions will result in stable long-term behavior due to the limit cycle, while the blue initial conditions will result in disastrous long-term behavior in the model. The bolded blue and yellow trajectories are where we outline the separatrices, dividing the phase plane plot into stable long-term behavior versus disastrous long-term behavior.

Note that mathematically, any initial conditions that fall within any of the yellow areas in Figure 5 will follow stable trajectories. In real-world terms, this means that any glacial levels and average radiation temperature conditions that fall within the yellow space will have little to no impact on the climate. Over the years, these levels will get closer and closer to the limit cycle, labeled in green in Figure 5. When values eventually flow to the limit cycle they will continue on this path. In real-world terms, once values continue on the limit cycle, this means that glacial levels and average radiation temperatures will increase and decrease slightly every few thousand years due to the natural, cyclic behavior of the Earth. On the other hand, any initial condition that falls within any of the blue areas in Figure 5 will follow unstable trajectories. In real-world terms, this means that any glacial levels and average radiation temperatures that fall within the blue space will

have significant impact to the climate.

In the next section, we will analyze the results of the phase plane plot by understanding the impacts of time.

4 Human Impact: Extending the Model to a New Millenium

In the remainder of this article, we reenvision the results of [6] by exploring the effect of human impact on the long-term behavior of the system. In the previous sections, we analyzed small changes in initial conditions with regard to the phase plane of each system. While the results of that exploration are significant, it is hard to understand how much time is involved with the potential dramatic changes caused by the effects of the saddle point. Instead of solely analyzing the phase plane, here we will evaluate state-time plots to help further understand the implications in real-world behaviors.

4.1 Cyclic Climate Behavior

We begin in (G, t) and (T, t) coordinates by showing in Figure 6 a stable trajectory that heads toward the limit cycle. The initial conditions used here are $(u_1, u_2) = (0, 1.5948)$, which translates to 9.672546% glacial volume and 246 K average radiation temperature. We have plotted $G(t)$ and $T(t)$ versus t. Note that this model shows periodic behavior for over $3,000,000$ years. Both T and G fluctuate throughout the years, but they do stay within their periodic bounds. This shows that the planet is remaining relatively stable and the climate change experienced here is purely natural. Note also that the fluctuations in G and T are more pronounced during the beginning of the trajectory and as time goes on, the fluctuations decrease and look like they become constant amplitude. This is the result of the trajectory aligning with the limit cycle and continuing on that path, theoretically, forever.

4.2 Slowly Changing Climate Behavior

The next plots display a 0.0001 change from the stable initial conditions to unstable initial conditions in u-coordinates, which translates to 9.672544% glacial volume and 246 K average global temperature. While this is a relatively subtle change in u-coordinates, the long-term behaviors in G and T are extreme as given in Figure 7. This initial condition does not head toward the limit cycle as seen in the previous plot in Figure 6. Instead, state-time curves head toward increasing changes in G and T that lead to drastic effects in the real-world. We have noted important milestones in the plots in Figure 7 that show when we have 5%, 3%, and 1% remaining glacial volume on the planet. We also have noted when the average radiation temperature of the planet increases to 333 K (equivalent to 60°C and 140°F), which creates unlivable human conditions. Note that the changes increase over time, they do not show periodic or cyclic naturally fluctuating behavior, and the time scale for drastic results appears less than 45,000 years.

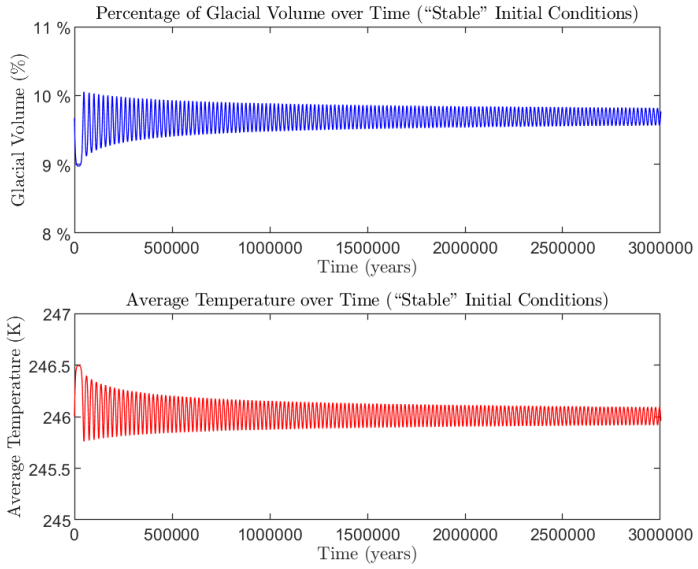

Figure 6: Percentage of glacial volume and average temperature of the planet over time using “stable" initial conditions in u-coordinates, (0,1.5948).

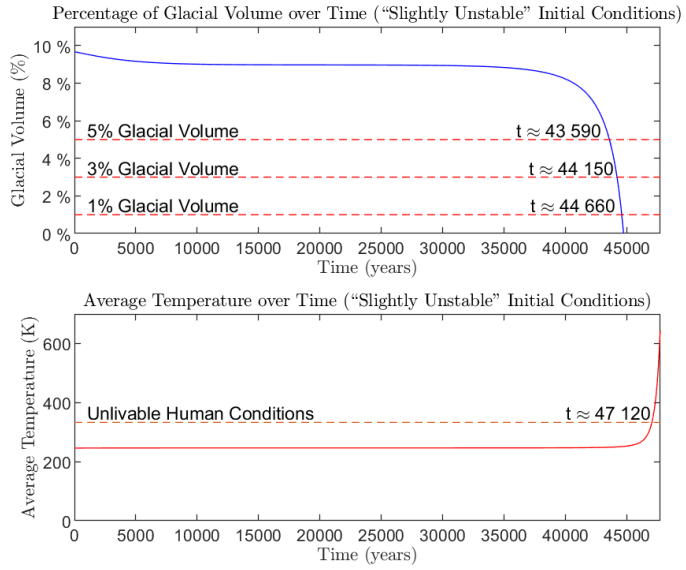

Figure 7: Percentage of glacial volume and average temperature of the planet over time using “slightly unstable” initial conditions in u-coordinates, (0,1.5949).

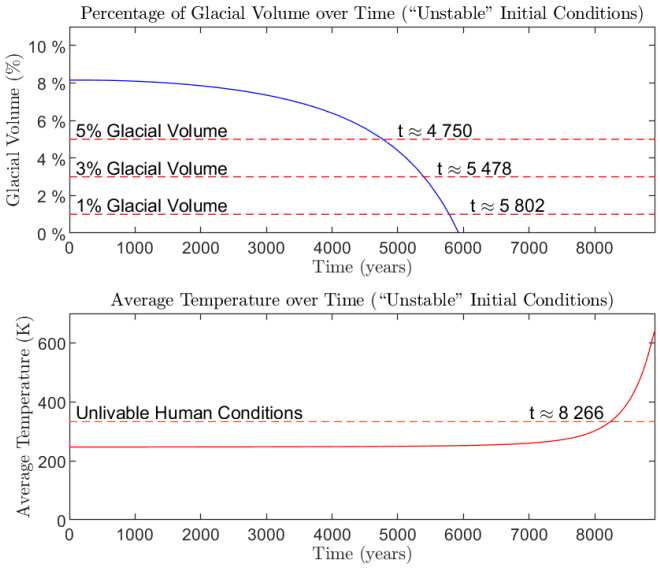

Figure 8: Percentage of glacial volume and average temperature of the planet over time using "unstable" initial conditions in u-coordinates, (5.6068,0).

4.3 Rapidly Deteriorating Climate Behavior

Initial conditions with a larger perturbation result in even more disaster. In the previous plot, we only had a minor change in u-coordinates. The initial conditions used here are $(u_1, u_2) = (5.6068, 0)$, which translates to 8.15152% glacial volume and 247.05 K average radiation temperature. The results are recorded in Figure 8. In this scenario, it only takes about $6,000$ years for the Earth to be depleted of its entire glacial volume.

4.4 Marker Plot

In the plots in Figures 9 and 10, we used markers to identify where the glacial volume and temperatures were every $10,000$ years for the stable model and every $1,000$ years for the unstable model. Note that for the stable model shown in Figure 9, Earth undergoes warming and cooling periods almost exactly every $10,000$ years. In the unstable version of this model shown in Figure 10, we can see that it takes some time before temperatures and glacial volume reach a turning point in the u-coordinate phase plane because trajectories slowly approach the saddle point before rapidly veering away to disaster. The differences between the behavior in Figure 9 and the behavior in Figure 10 could not be more stark.

5 Discussion

The toy climate model from [6] is just that—a toy model. However, it brings many fundamental principles of climate science to life. Building this model mathematically allowed us to understand the impacts on both glacial volume and average planetary

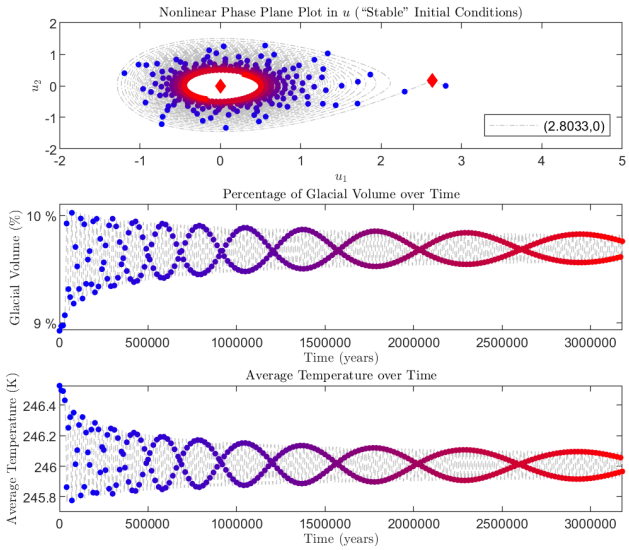

Figure 9: Percentage of glacial volume and average temperature of the planet over time using "stable" initial conditions in u-coordinates, (2.8033,0), where markers are displayed every 10,000 years. Marker colors provide reference to time in the top plot for the G and T phase plane.

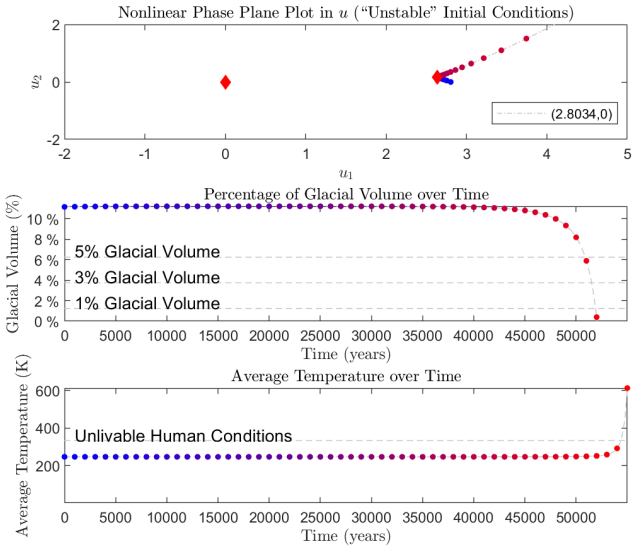

Figure 10: Percentage of glacial volume and average temperature of the planet over time using "unstable" initial conditions in u-coordinates, (2.8034,0), where markers are displayed every 1,000 years. Marker colors provide reference to time in the top plot for the G and T phase plane.

temperature through various initial conditions. By understanding the relationship between u-coordinates and (G, T)-coordinates, we were able to translate the results into real-world meaning.

When "stable" initial conditions in u-coordinates were used that had trajectories that headed toward the limit cycle, the model outputted values for more than three million years, and while there were minor perturbations, G and T remained relatively stable over the time period. This represents the natural fluctuations the earth goes through over a long period of time, independent of human activity.

When "slightly unstable" initial conditions in u-coordinates were used that had trajectories to mimic the changes human activity may have influenced in the model, we saw dramatic differences in the model output. Even though these initial conditions varied by only 0.0001 units in u as compared to the initial conditions that headed toward the limit cycle, the results showed that even a slight change created dramatic impacts on the climate. For all model scenarios, at around $50,000$ years, we completely depleted our resource in glaciers. This caused the temperature to increase dramatically and quickly caused unlivable human conditions where the average radiation temperature of the planet was 333 K, approximately 140° Farenheit.

Finally, rather than slight, minuscule changes in u-coordinates, we considered initial conditions sufficiently far out and observed even more drastic behavior. In this scenario, using initial conditions from the right side of the saddle resulted in only $6,000$ years—less than half of the time it took in the "slightly unstable" version—until the complete depletion in glacial volume and unlivable temperatures for humans. This is an incredibly grim timeline that is being reflected from extreme human interaction.

If, as most scientists believe, human activity is changing our climate, it is not far-fetched to view this human-driven effect as changing the initial conditions in the present time. Our results, though obtained from a toy model, suggest that the outcome may be disastrous for humanity if we reach a point of no return. To conclude on a more hopeful note, if humanity can change the initial conditions in the present time for the worse, humanity can also choose to change the initial conditions in the present time for the better.

References

[1] John Kroll. Fire, ice, water, and dirt: A simple climate model. *Chaos: An Interdisciplinary Journal of Nonlinear Science*, 27(7):073101, 2017. https://doi.org/10.1063/1.4991383.

[2] Erics Posmentier. Periodic, quasiperiodic, and chaotic behaviour in a nonlinear toy climate model. In *Annales Geophysicae*, volume 8, pages 781–790, 1990.

[3] Barry Saltzman, Alfonso Sutera, and Alan Evenson. Structural stochastic stability of a simple auto-oscillatory climatic feedback system. *Journal of the Atmospheric Sciences*, 38(3):494–503, 1981.

[4] Peter T Saunders. Evolution without natural selection: further implications of the daisyworld parable. *Journal of Theoretical Biology*, 166(4):365–373, 1994.

[5] Michael S Toner. *Invariant manifolds of a toy climate model*. PhD thesis, Old Dominion University, 1994. https://doi.org/10.25777/w41a-bm34.

[6] Michael S Toner and AD Kirwan Jr. Periodic and homoclinic orbits in a toy climate model. *Nonlinear Processes in Geophysics*, 1(1):31–40, 1994.

[7] Andrew J Watson and James E Lovelock. Biological homeostasis of the global environment: the parable of daisyworld. *Tellus B: Chemical and Physical Meteorology*, 35 (4):284–289, 1983.

[8] Andrew J Wood, Graeme J Ackland, James G Dyke, Hywel TP Williams, and Timothy M Lenton. Daisyworld: A review. *Reviews of Geophysics*, 46(1), 2008. https://doi.org/10.1029/2006RG000217.